Electric-Field-Induced Actuation of Poly(vinyl alcohol) Microfibers

ARTICLE *in* THE JOURNAL OF PHYSICAL CHEMISTRY C · NOVEMBER 2012

Impact Factor: 4.77 · DOI: 10.1021/jp306979c

3 AUTHORS, INCLUDING:

Hong Xia
Shinshu University, Ueda, Japan
14 PUBLICATIONS **51** CITATIONS
SEE PROFILE

Toshihiro Hirai
Shinshu University
197 PUBLICATIONS **1,472** CITATIONS
SEE PROFILE

THE JOURNAL OF PHYSICAL CHEMISTRY C

Article

pubs.acs.org/JPCC

Electric-Field-Induced Actuation of Poly(vinyl alcohol) Microfibers

Hong Xia,[†] Yoshio Hashimoto,[‡] and Toshihiro Hirai*[,†]

[†]Smart Materials Engineering, Faculty of Textile and Technology, Shinshu University, 3-15-1 Tokida, Ueda, Nagano 386-8567, Japan

[‡]Department of Electrical and Electronic Engineering, Faculty of Engineering, Shinshu University, 4-17-1 Wakasato, Nagano, Nagano 380-8553, Japan

Supporting Information

ABSTRACT: Poly(vinyl alcohol) (PVA) microfibers were actuated by application of a direct current (dc) electric field; there were large electrosensitivity differences between water-soluble and high-tenacity fibers. In particular, a bending actuation was observed for water-soluble PVA fibers with high sensitivity and large deformation upon applying a dc electric field. The mechanism of bending actuation was investigated through analysis of the chemical constituents, dielectric properties, bending rigidity, and morphology. It was found that the actuation behavior depends mainly on the mechanical and dielectric properties, which are related to the chemical structures of the fibers. It is clear that hydroxyl and carbon−oxygen double bonds are key factors influencing the electroactive characteristics. The content of hydroxyl groups not only determines the solubility of PVA fibers in water but also controls the antielastic bending. The content of C═O groups may be related to the dielectric constant and bending rigidity. Furthermore, the C—S bond in the X-ray photoelectron spectrum indicates that dimethyl sulfoxide remains even after solvent removal, and this can make it easier for the PVA fibers to become positively charged and then bend toward the cathode.

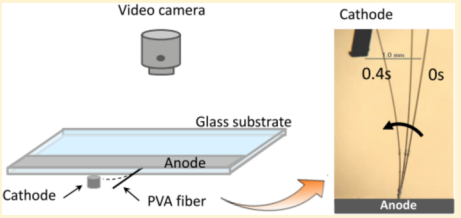

1. INTRODUCTION

Electroactive polymers (EAPs) are the best-known examples of polymer actuator materials and have been widely used in biomimetic artificial muscle.[1−4] Poly(vinyl alcohol) (PVA) is an EAP polymer with good thermal stability, chemical resistance, water permeability, and biocompatibility,[5−7] and it is widely used in the plastics, fiber, and textile industries. PVA has also attracted attention as a high-performance polymer in the emerging field of actuator materials since Hirai et al. found, over 20 years ago, that a PVA/dimethyl sulfoxide (DMSO) gel could be actuated by applying an electric field.[8−12] PVA/DMSO gels that are swollen with a large amount of DMSO solvent (about 98 wt %) are asymmetrically electrically deformed by solvent drag. DMSO induces PVA gels to bend or crawl from the anode to the cathode[13,14] because DMSO is a polar aprotic solvent (with a high dielectric constant), and orients along the direction of the electric field.[15] This development has attracted widespread attention in various fields for use in biomimetic materials, artificial muscles, and other applications.

Recently, many researchers have explored the spinning of high-strength PVA fibers using various methods. Gel-spun fibers,[16,17] cross-linked wet-spun fibers,[18,19] and zone-drawn fibers[20,21] have all been studied. In 1998, Kuraray Co., Ltd. (Tokyo, Japan), developed a new PVA fiber, called KURALON K-II, produced using the wet cooled-gel spinning method.[22−24] Glycerine, pure DMSO, and DMSO/H_2O were used as solvents in studies of PVA fiber spinning; no major differences in the final fiber strengths were found for these three solvents. For ease of solvent removal from the gelled PVA, pure DMSO was adopted for making PVA fibers. There are two types of KURALON K-II: a water-soluble type, which is soluble in water at normal temperatures, and a high-tenacity type, which is soluble at high temperatures (≥100 °C). The former is blended with wool or cotton to make clothing, and the latter is used as a reinforcing material for pillars, walls, bridges, and railway lines.

The study of electroactive fibers (EAFs) is a new challenge in terms of actuator materials since fibers have specific structures, and are easily fabricated into thin, uniform, and functional actuator materials for applications such as artificial skin, blood vessels, and muscles, and in tissue engineering. The development of new EAFs is therefore an important topic. However, the actuation of polymer-based fibers is poorly understood and has been little investigated, to the best of our knowledge.

In this study, PVA fibers were used, and their electrical actuation behaviors were investigated by application of an electric field. Water-soluble and high-tenacity fibers were used. During spinning of the PVA fibers, pure DMSO was used as the solvent, and this greatly influenced the fiber properties. Four types of PVA fiber, with different amounts of DMSO solvent and different degrees of saponification (DS), were used to investigate the relationship between the actuation characteristics and the molecular structures of the fibers. A direct current (dc) electric field was applied to determine and compare the electrical response abilities of the PVA fibers. The relationships between chemical composition and structure and dielectric and mechanical properties were also investigated using X-ray photoelectron spectroscopy (XPS), dielectric constant measurements, and pure bending experiments. Our aim was to clarify the actuation mechanisms of PVA fiber and find the optimal conditions for PVA fiber actuation.

Received: July 13, 2012
Revised: September 3, 2012
Published: October 5, 2012

2. EXPERIMENTAL SECTION

2.1. Materials. Four types of PVA fiber (three water-soluble and one high-tenacity type) were provided by Kuraray Co., Ltd. DMSO was used as the solvent in the spinning process. The dissolution temperatures of the PVA fibers in water were 20, 40, 70, and ≥100 °C, and their deniers were 2.2, 1.4, 2.2, and 2.0 dtex; the four fibers were coded as samples A, B, C, and D (as shown in Table 1). The chemical structure is as follows.

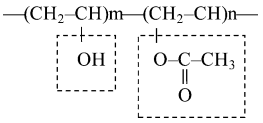

2.2. Actuation of Fibers. The set up for fiber actuation is shown in Figure 1a. The fiber was nipped on the anode, and the cathode was set near the fiber tip, 1 mm from the tip of the fiber, as in a cantilever bending test. When a dc electric voltage was turned on at 1 kV, the tip of the fiber was attracted toward the cathode and a video camera on a microscope recorded the fiber bending process in real time (Figure 1b). We also examined the actuation of PVA fibers using different boundary support conditions.

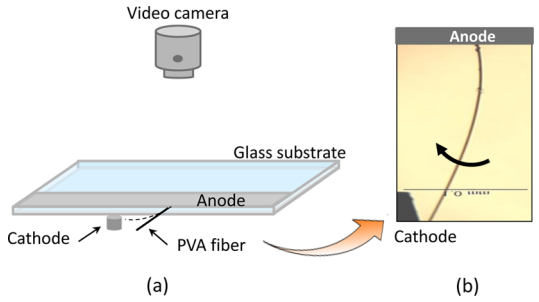

Figure 1. Fiber actuation tests by applying an electric field: (a) set up of fiber actuation test and (b) bending actuation image for a single fiber clamped at the anode like a cantilever.

2.3. Pure Bending Test. A KES-FB2 pure bending tester (KATA Tech Co., Ltd., Japan) was used to evaluate the bending rigidity of PVA fibers and to investigate the relationship between bending properties and electrically induced actuation. An equal number of 3-cm lengths of fibers were uniformly fixed between two chucks and bent in an arc of constant curvature, which was changed continuously (deformation speed: 0.5 cm/s). The bending moment limit of the sample was determined, and the relationship between the bending moment and the curvature for a single bending cycle was then recorded.

2.4. XPS Analysis. An AXIS-ULTRA DLD high-performance X-ray photoelectron spectrometer (KRATOS) with nonmonochromatized Mg Kα X-rays in high-energy mode was used to study the chemical compositions and bonding states of the PVA fibers and to investigate the effects of these properties on the electric-field-induced fiber actuation. The energy resolution was set with 1-eV steps and a 160-eV range for wide scans, and 0.1-eV steps and a 40-eV range for narrow scans. With an XPS peak-fitting program (XPSPEAK Ver.4.1, Dr Kwok), the peaks from C1s were fitted with a Gaussian–Lorentzian product function. The C1s and O1s binding energies (BEs) of the PVA peaks were fixed at 284.6 and 532.2 eV to calibrate the BE scales.

2.5. Scanning Electron Microscope (SEM) Observations and Impedance Analyses. A Solartron 1260/1296 dielectric impedance measurement system (Toyo Technical, Ltd., Japan) with a frequency response analyzer was used to evaluate the interfacial characteristics, molecular interactions, and polarization via impedance spectra measurements. The samples were measured over the frequency range 10^0–10^6 Hz with 100 mV at room temperature. Because of the very narrow potential range used, ac impedance is minimally destructive to the measured sample.[25]

SEM (S-3000N, Hitachi) combined with an energy-dispersive X-ray spectrometer (EDX, Horiba) was used to observe and analyze the morphologies and surface elements in different parts of the fibers.

Table 1. Comparison of PVA Fibers of Different Types and with Various Parameters

	water-soluble			high-tenacity
	sample A	sample B	sample C	sample D
dissolution temp (°C)	20	40	70	≥100
deniers (dtex)[a]	2.2	1.4	2.2	2.0

[a]dtex = 1 gram mass of fiber in grams per 10 000 m length.

3. RESULTS AND DISCUSSION

3.1. Actuation of PVA Fibers by Applying an Electric Field. PVA fibers of length 3 mm were made to bend in different ways by changing the boundary support conditions (edge setting conditions), as shown in Figure 2a,c,d. Figure 2a shows a single PVA fiber from sample A actuated by an electric

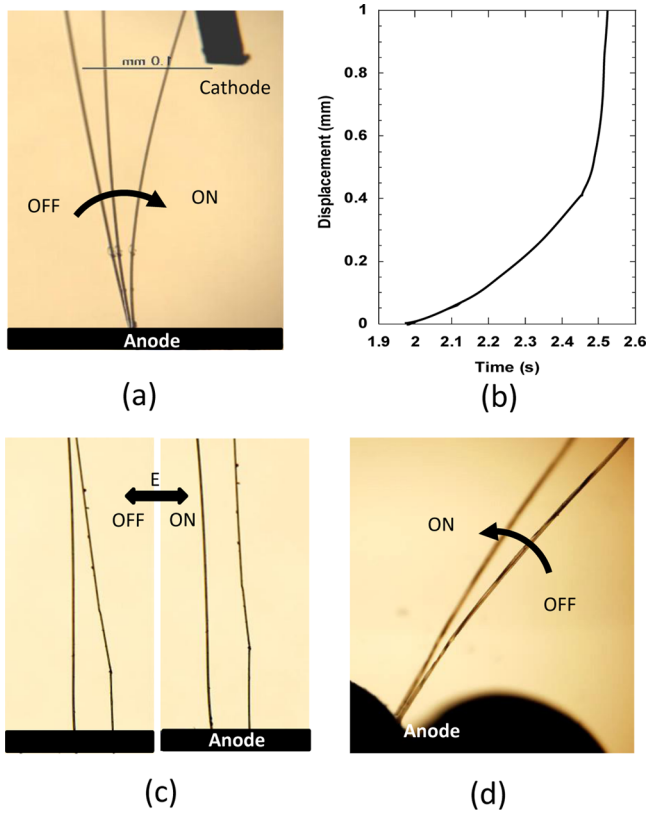

Figure 2. Actuations of PVA fibers induced by applying a 1-kV dc electric field under different boundary support conditions: (a) bending process for a single fiber clamped at the anode, (b) curve of fiber tip displacement with activity time of electric field, (c) two fibers separately set at the anode, and (d) two fibers twisted together and set at the anode.

dx.doi.org/10.1021/jp306979c | J. Phys. Chem. C 2012, 116, 23236–23242

field of 1 kV. When the electric field was switched from OFF to ON, a fiber with one end fixed like a cantilever bent to the cathode side and the fiber tip moved to the cathode with increasing time. The relationship between fiber tip displacement and time is shown in Figure 2b, and the slope of the curve gives the time dependence of the electric-field-induced actuation. The fiber tip displacement reached 1 mm (attached to the cathode) within 0.4 s.

Figure 2c shows the actuation of PVA fibers interfering with each other. Two fibers from sample A were separately fixed at one end with the fiber tips in contact with each other. When an electric field was applied, the two fibers separated because of repulsion caused by the positive charges on the fibers. Figure 2d shows the actuation of a twisted fiber, in which two fibers are twisted together. The induced electric field causes the twisted fibers to move to one side. The two fibers could not be separated because of the twisting, so they move as one fiber. The actuation of the twisted fiber will depend on the fiber properties of each component fiber and of the twisted structure. The actuation characteristics of the PVA fibers therefore depend not only on the fiber structure but also on their boundary support conditions. The positively charged fibers were either attracted to the cathode or repulsed by each other upon application of a dc electric field. Because the fineness and twisting of the fibers are not uniform, the fibers may generate a power disparity when they push each other. Their displacements were therefore different, or they bent to one side, i.e., the weaker side (as shown in Figures 2c and 3d). Videos of the PVA fiber actuation process are shown in Supporting Information S1–S3. For the PVA fibers, the DMSO solvent is a key component. In the actuation mechanism of the PVA fibers, the DMSO made positive charging of the fibers easy, and therefore, they bent toward the cathode; this is because DMSO is a polar aprotic solvent with a high dielectric constant. The bending mechanism is shown in Figure 3.

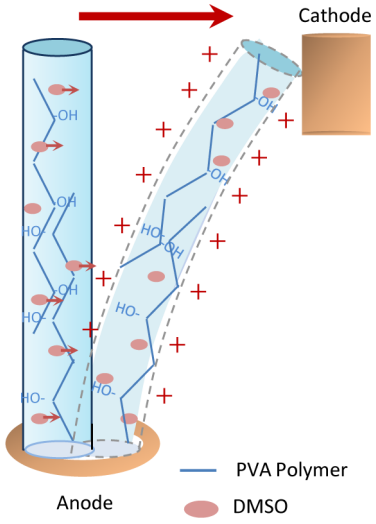

Figure 3. Schematic illustration of bending mechanism for a single PVA microfiber by electric stimulation.

Figure 4 shows the fiber tip displacements with time of single fibers, set as in Figure 2a with one end fixed, of the four PVA samples A, B, C, and D, when the 1-kV dc electric field was switched on and off. Sample A (red line) bent fastest; samples B and C (blue and black lines) bent in a similar way (the fiber tip arrived at the cathode within 6–8 s of switching on the

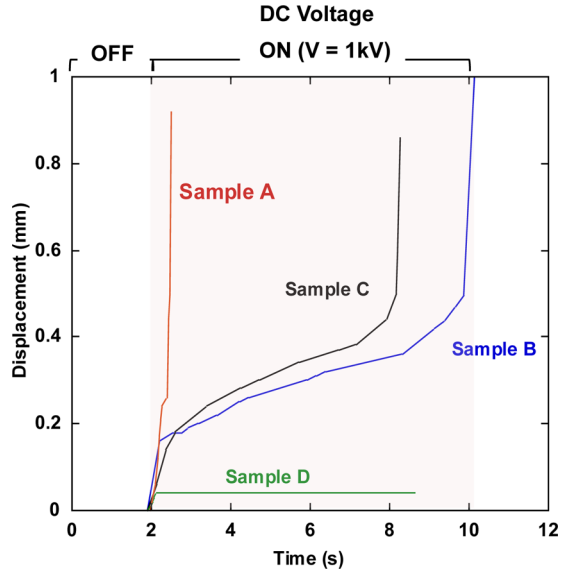

Figure 4. Fiber tip displacements with time for sample A, B, C, and D fibers, set as in Figure 2a, when a 1-kV dc electric field was turned ON and OFF.

electric field). Sample D (green line) was the slowest during bending; the fiber tip displacement was about 0.04 mm, and the fiber did not attach to the cathode. We can therefore see that, for the water-soluble PVA fibers (samples A, B, and C), the actuation displacement was large enough for the fibers to reach the cathode, whereas for the high-tenacity type PVA fiber (sample D), the actuation displacement was small. It is considered that the different actuation characteristics of these PVA fibers are related to their physical properties and chemical structures.

3.2. SEM Observations. Figure 5 shows SEM images of four PVA fibers. Fibers A, B, and C present a smooth and

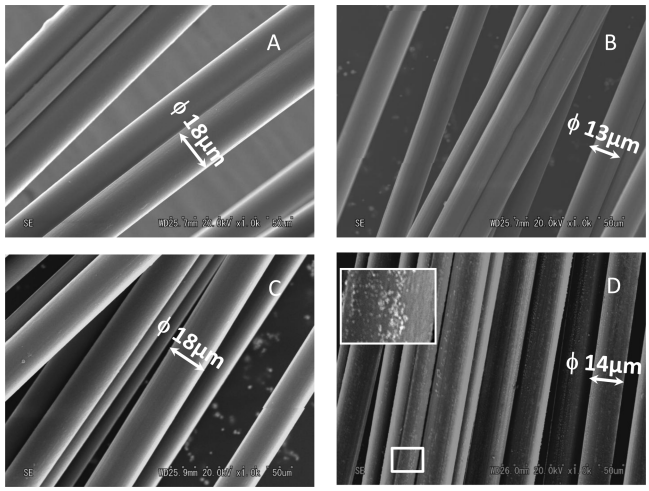

Figure 5. SEM images of four PVA fibers: (a) sample A, (b) sample B, (c) sample C, and (d) sample D. The inset is a higher magnification image of the area in the white frame.

uniform surface, whereas fiber D shows a rougher surface with many small particles. The compositions of the powders are the same as those of the fiber main body, as assessed by EDX analysis. The diameters of fibers A and C are 18 μm, that of fiber B is 13 μm, and that of fiber D is 14 μm.

dx.doi.org/10.1021/jp306979c | J. Phys. Chem. C 2012, 116, 23236–23242

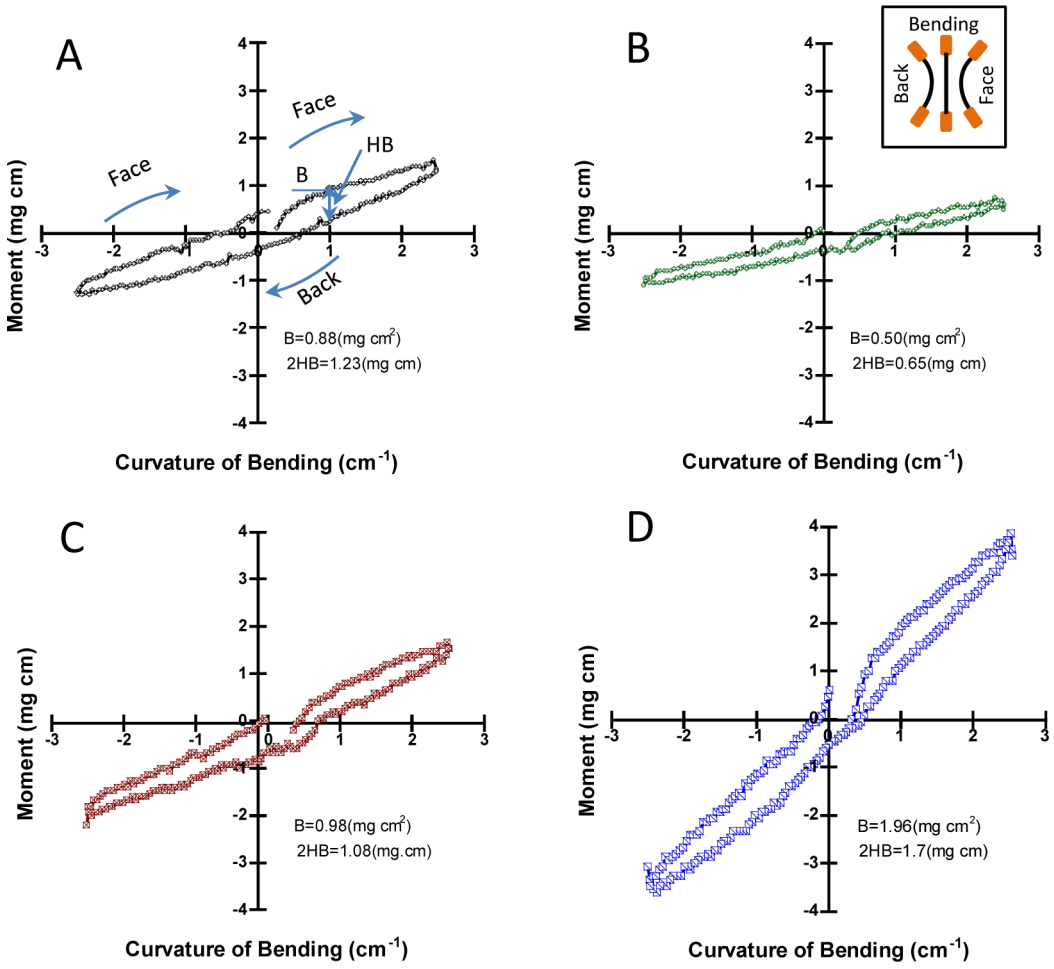

Figure 6. Results of pure bending measurements for the four PVA fiber samples: (a) sample A, (b) sample B, (c) sample C, and (d) sample D. The inset shows the fiber bending method.

3.3. Bending Properties. The results of the bending tests for the PVA fibers are shown in Figure 6. The samples were bent in an arc which started near the origin of the coordinates, passed the bending maximum, and then returned to the starting point, with the curvature changing continuously. The parameters used to evaluate the bending properties of the PVA fibers were bending rigidity (B), which was measured from the mean slope in the range $K = 0.5-1.5$ cm^{-1} (K is curvature), and the hysteresis of bending moment ($2HB$), which was measured at $K = 1.0$ cm^{-1}. The values were obtained using the following formulas:[26,27]

$$M = B(K \pm HB) \quad (1)$$

$$B = (B_f \pm B_b)/2B \quad (2)$$

$$2HB = (HB_f \pm HB_b) \quad (3)$$

where M is the bending moment, B_f and B_b are bending rigidities, and HB_f and HB_b are hysteresis of bending moments for face and back bending.

In Figure 6, PVA fiber D shows the largest bending rigidity, 1.96 mg cm^2, and a hysteresis of bending moment of 1.7 mg cm. This means that fiber D is the hardest of the four PVA fibers, and has lower antielastic bending than the other fibers. The displacement of fiber D was the smallest in the actuation tests when an electric field was applied. Fiber B has a bending rigidity of 0.5 mg cm^2 and a hysteresis of bending moment of 0.65 mg cm, and is the softest fiber. Although the diameters of fibers B and D are similar, there is an approximately 3-fold difference between their bending rigidities and their hysteresis of bending moments. This results in a large difference between the actuation displacements for these two fibers, as a result of their different structures, i.e., water-soluble and high-tenacity type, respectively. A comparison of the three water-soluble fibers A, B, and C shows that the bending rigidity of fiber A is 0.88 mg cm^2, a little lower than that of fiber C (bending rigidity of 0.98 mg cm^2), but the antielastic bending of fiber C ($2HB$ = 1.08 mg cm) is better than that of fiber A ($2HB$ = 1.23 mg cm). This may be related to the chemical compositions, e.g., the number of hydroxyl groups (−OH); this will be discussed later.

3.4. Dielectric Properties. In complex impedance diagrams, as shown in Figure 7c, the imaginary part of the impedance Z'' (ohms) is plotted against the real part Z' (ohms). The response of an ideal parallel circuit of resistance R and capacitance C is a semicircle centered on the Z' axis. R is determined from the diameter of the semicircle, and C is calculated from the frequency of the maximum of the semicircle.[28]

The impedance responses of four PVA fibers are shown in Figure 7c. The diameters of the semicircles correspond to the interfacial resistances of the PVA fibers and electrodes. The interfacial resistance of fiber D was much larger than that of the other fibers. The real part (ε') and imaginary part (ε'') of the dielectric constants of the four fibers are shown in Figure 7a,b.

dx.doi.org/10.1021/jp306979c | J. Phys. Chem. C 2012, 116, 23236−23242

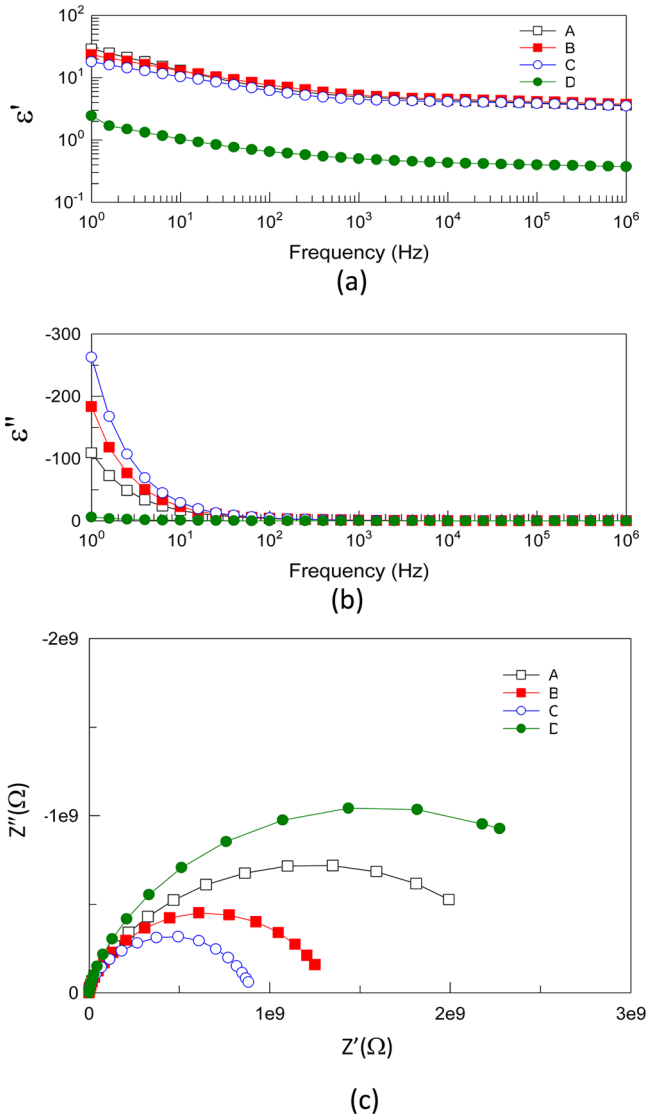

Figure 7. Impedance results for four fiber samples: (a and b) the real and imaginary components of the dielectric constant and (c) Cole–Cole plots of the PVA fibers.

The dielectric response of the PVA microfibers can be succinctly described by expressing the relative dielectric constant as a complex quantity made up of a real component and an imaginary component:

$$\varepsilon^* = \varepsilon' - i\varepsilon'' \quad (1)$$

The dielectric constants (ε' and ε'') represent the amount of energy storage and energy loss in a dielectric material, respectively.[29] The real (ε') and imaginary (ε'') parts of the dielectric constant were calculated from the formulas

$$\varepsilon' = \frac{Cd}{\varepsilon_o A} \quad (2)$$

$$\varepsilon'' = \varepsilon' \tan \alpha \quad (3)$$

where C is the capacitance and ε_0 is the vacuum dielectric constant. A and d are the area and separation of the electrodes, respectively, and tan α is the dielectric loss. In Figure 7a, the dielectric constant (ε') of fiber D is substantially lower than that of the other fibers. This is related to the poor actuation behavior of fiber D. The imaginary part of the dielectric constants (ε'') of the four fibers is shown in Figure 7b. Among the three water-soluble PVA fibers, fiber A displays the highest dielectric constant (ε') and the lowest energy loss (ε'') at low frequency. Fiber A therefore shows a superior actuation ability upon application of an electric field.

3.5. Analysis of Chemical Composition. The chemical compositions and structures determine the actuation characteristics of PVA fibers; XPS helps us to understand the chemical compositions and interactions of the fiber samples. Figure 8 shows the XPS spectra of PVA fibers A, B, C, and D, obtained using a nonmonochromatic Mg Kα X-ray source. The overall and C1s regions, with the fitting details, are shown in parts A1–D1 and A2–D2, respectively. Table 2 lists the parameters of each XPS spectrum, such as chemical shift (eV), full-width at half-maximum (eV), and relative area (%).

Wide-Scan Region. The top row in Figure 8 shows the wide-scan spectra for the PVA fibers. As well as oxygen and carbon, silicon and phosphorus elements were found in fiber A, and small amounts of sulfur and silicon were found in fiber D (as shown in the insets). Silicon and phosphorus are present because silicon and phosphorus compounds were added as cross-linking and flame retardant agents in the spinning process. The sulfur is most likely from residual DMSO.

C1s Core Level. The bottom row of Figure 8 shows the high-resolution spectra of the C1s core level (scanned with a step one-tenth that of the wide scan) and the fitted curves used to determine the chemical bonding. The C1s region could be fitted by four peaks. Peak 1 (284.6 eV) and peak 4 (287 ± 0.3 eV) correspond to C—C, C—H, and C═O group. Peaks 2 (285.8 ± 0.2 eV) and 3 (286.6 ± 0.2 eV) correspond to C—OH groups and groups containing C with S.[30−34]

The relative area of peak 2 (C—OH) was smaller than those for fibers A–C, as shown in Table 2. The amount of hydrophilic groups (OH) in peak 2 correlates with the dissolution temperature in water for the water-soluble PVA fibers. It might be expected that PVA fibers containing many hydroxyl groups would dissolve more easily in water. However, although fiber D contains the most hydroxyl groups, it is difficult to dissolve in water because there are many strong hydrogen bonds in the molecular structure.[22,23] Furthermore, the content of hydroxyl groups will influence the moisture content of PVA fibers, which may affect the bending rigidity and antielastic behavior.

Peak 3 (C–S) reflects the content of residual DMSO molecules in the fibers after solvent removal. Going from PVA fibers A–D, the relative area of peak 3 (C–S) increased; fiber A displayed the best actuation properties, fiber D showed the smallest response, and fibers B and C displayed intermediate responses to electrical stimulation. DMSO plays an important role by forming PVA/DMSO compounds, especially in PVA gels. DMSO can easily promote positive charging of the PVA polymer, but the DMSO contents at different water ratios or concentrations of cross-linking agent have different influences on the mechanical and dielectric properties of the resultant materials.[35,36]

Peak 4 (C═O) represents the side group (acetate) content, and C═O bonds are highly polar. This is reflected not only in the molecular structure, but also influences the dielectric properties of the PVA fibers. In Figure 8, the area ratios of peak 4 are similar (about 5%) for fibers A, B, and C. This suggests that there are no large differences among their dielectric constants. The hydroxyl group is also a polar bond, but it is much weaker than C═O. There are therefore only small differences among the dielectric characteristics of fibers A, B, and C. For fiber D, peak 4 (C═O) did not appear. This is consistent with fiber D

dx.doi.org/10.1021/jp306979c | J. Phys. Chem. C 2012, 116, 23236–23242

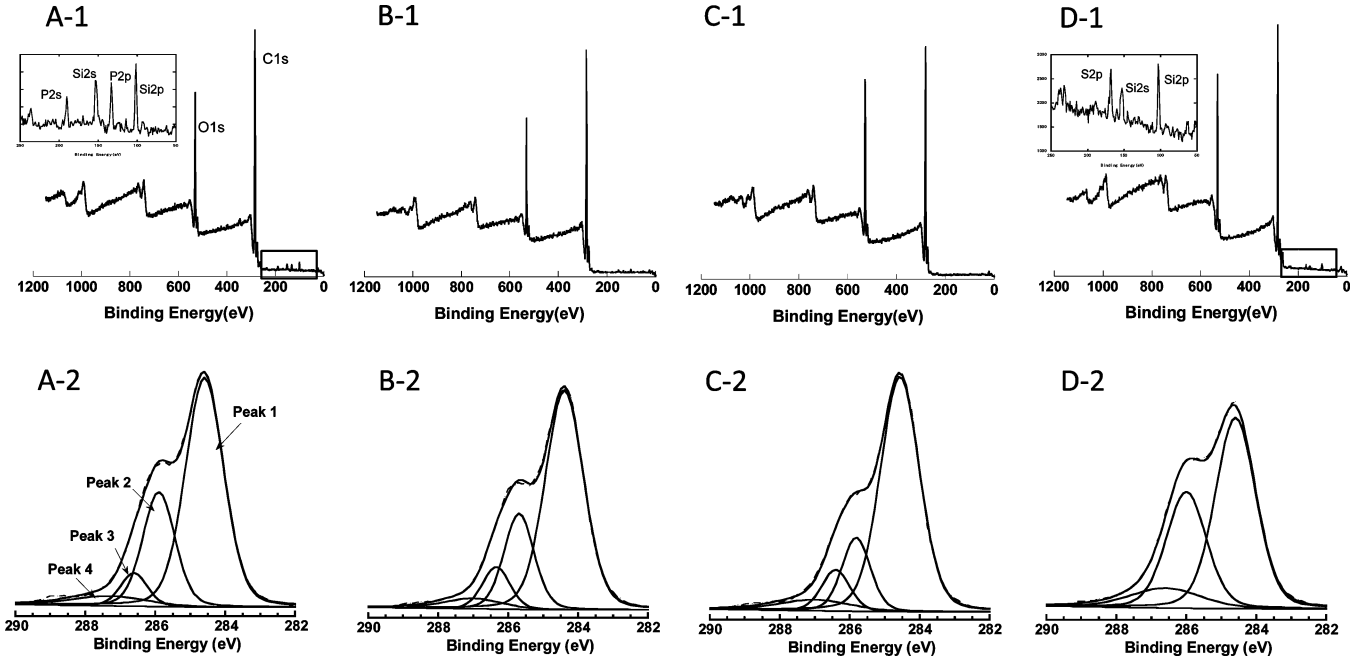

Figure 8. XPS spectra of PVA fibers. Wide scans are shown in A-1 to D-1, and C1s regions in A-2 to D-2. The insets are magnifications of the circled regions (binding energy 50−250 eV).

Table 2. Parameters of C1s XPS Spectra of PVA Fibers

		C1s (A-2)			C1s (B-2)			C1s (C-2)			C1s (D-2)		
	chemical bonds	B.E. (eV)	fwhm	area (%)	B.E. (eV)	fwhm	area (%)	B.E. (eV)	fwhm	area (%)	B.E. (eV)	fwhm	area (%)
peak 1	C−C, C−H	284.6	1.29	62.29	284.4	1.29	64.67	284.6	1.31	69.49	284.6	1.36	56.05
peak 2	C−OH	285.9	1.09	26.21	285.7	1.01	22.13	285.8	0.96	15.85	286	1.35	33.84
peak 3	C−S	286.6	0.9	6.32	286.4	0.91	8.56	286.4	0.94	8.72	286.6	2.37	10.12
peak 4	C═O	287.3	2.49	5.17	287	1.95	4.64	287	2.4	5.95			

having an extra-high DS (almost no acetate side groups), and a highly crystalline molecular structure. Fiber D therefore has the greatest bending rigidity and the lowest dielectric constant of these four PVA fibers.

It is clear that all these bonds in the fiber structures resulted in different actuation characteristics of the PVA fibers.

4. CONCLUSION

Excellent actuation of electroactive PVA microfibers was found in this work. In particular, water-soluble PVA fibers bent with high sensitivity and large deformation upon application of a dc electric field in air.

The mechanism of bending actuation was investigated through analysis of the chemical constituents, dielectric properties, bending rigidities, and morphologies. It was found that the actuation behavior depended mainly on the mechanical and dielectric properties, which are related to the chemical structures of the fibers. It is clear that hydroxyl and carbon−oxygen double bonds are important factors influencing the electroactive characteristics of PVA fibers. The content of hydroxyl groups not only determines the solubility of the PVA fiber in water but also controls the antielastic bending. The content of C═O groups may control the PVA crystallinity, dielectric constant, and bending rigidity. For PVA fibers that dissolve easily in water, adding cross-linking agents or flame retardants not only improved their mechanical properties and fire resistance but also improved their actuation properties. Peak 3 (C—S) in the XPS indicates that some DMSO remains even after solvent removal. The remaining DMSO made it easier for the PVA fibers to become positively charged and then bend toward the cathode.

The results demonstrate the actuation mechanism and its relationship with the chemical, mechanical, and dielectric properties of PVA fibers. This electric-field-induced actuation of PVA microfibers is expected to have various applications in biomimetic materials, artificial muscles, and interface materials.

■ ASSOCIATED CONTENT

Ⓢ Supporting Information

Videos (S1−S3) for the actuation of electroactive PVA microfibers. This material is available free of charge via the Internet at http://pubs.acs.org.

■ AUTHOR INFORMATION

Corresponding Author

*E-mail: tohirai@shinshu-u.ac.jp.

Notes

The authors declare no competing financial interest.

■ ACKNOWLEDGMENTS

We are grateful to Kuraray Co., Ltd., for providing samples of PVA fibers.

■ REFERENCES

(1) Osada, Y.; Danilo De Rossi, E., *Polymer Sensors and Actuators*, Springer: New York, 2000; pp 245−255.

(2) Carpi, F.; Smela, É. *Biomedical Applications of Electroactive Polymer Actuators*; Wiley: London, 2009; pp 1−4.
(3) Bar-Cohen, Y. *Electroactive Polymer (EAP) Actuators as Artificial Muscles: Reality, Potential, and Challenges*; SPIE: Washington, DC, 2004; pp 1−50.
(4) Bar-Cohen, Y. *Artificial Muscles using Electroactive Polymers (EAP): Capabilities, Challenges and Potential*; website http://ndeaa.jpl.nasa.gov; pp 1−14.
(5) Young, T. H; Chuang, W. Y. S. *J. Membr. Sci.* **2002**, *210*, 349−359.
(6) Wong, K. K. H.; Martin, Z. A.; Wan, W. k. *J. Mater. Sci.* **2010**, *45*, 2456−2465.
(7) Sakurada, I. *Polyvinyl Alcohol Fibers*; Marcel Dekker: New York, 1985.
(8) Zheng, J. M.; Watanabe, M.; Shirai, H.; Hirai, T. *Chem. Lett.* **2000**, *29*, 500−500.
(9) Hirai, T.; Ueki, T.; Takasaki, M. *JFBI* **2008**, *1*, 1−6, , http://www.jfbi.org/admin/Issue/JFBI%20Vol%201,%20No.%201,%20June%202008_20081022224820_paper.pdf.
(10) Hirai, T.; Nemoto, H.; Hirai, M.; Hayashi, S. *J. Appl. Polym. Sci.* **1994**, *53*, 79−84.
(11) Hirai, T. *J. Intell. Mater. Syst. Struct.* **2007**, *18*, 117−122.
(12) Hirai, T.; Nemoto, H.; Suzuki, T.; Hayashi, S.; Hirai, M *J. Intell. Mater. Syst. Struct.* **1993**, *4*, 277−279.
(13) Liang, S. M.; Xu, J.; Weng, L. W.; Zhang, L. N.; Guo, X. L.; Zhang, X. L. *J. Phys. Chem. B* **2007**, *111*, 941−945.
(14) Hirai, T.; Zheng, J. M.; Watanabe, M. *Proc. SPIE* **1999**, *3669*, 209−217.
(15) Hirai, T., Zheng, J. M., Watanabe, M.; Shirai, H. *Smart Fibres, Fabrics and Clothing*; Tao, X. M., Ed.; Woodhead Publishing: Cambridge, U.K, 2001; Chapter 2.
(16) Cebe, P.; Grubb, D. *J. Mater. Sci.* **1985**, *20*, 4465−4478.
(17) Grubb, D. T.; Kearney, F. R. *J. Appl. Polym. Sci.* **1990**, *39*, 695−705.
(18) Fujiwara, H.; Shibayama, M.; Chen, J. H.; Nomura, S. *J. Appl. Polym. Sci.* **1989**, *37*, 1403−1414.
(19) Hwang, K. S.; Lin, C. A.; Lin, C. H. *J. Appl. Polym. Sci.* **1994**, *52*, 1181−1189.
(20) Garrett, P. D.; Grubb, D. T. *J. Polym. Sci., Part B: Polym. Phys.* **1988**, *26*, 2509−2523.
(21) Kunugi, T.; Kawasumi, T.; Ito, T. *J. Appl. Polym. Sci.* **1990**, *40*, 2101−2112.
(22) Ohmori, A. *J. Text. Mach. Soc. Jpn.* **1997**, *50* (1), 52−55, , https://www.jstage.jst.go.jp/article/transjtmsj1972/50/1/50_1_P52/_article.
(23) Ohmori, A.; Sakuragi, I.; Onodera, M. Journal of the Society of Fiber Science and Technology, Japan. **1999**, *55* (12), 418−422.
(24) Hikasa, J. Fibers, Poly(vinyl alcohol). *Kirk-Othmer Encyclopedial Chemical Technology*; John Wiley & Sons: Hoboken, NJ, 2007; pp 1−12.
(25) Hirai, T., Xia, H. Hirai, K. IEEE ICMA, 2010, 71−76; http://ieeexplore.ieee.org/search/freesrchabstract.jsp?tp=&arnumber=5587920.
(26) Kawabata, H. *The Standardisation and Analysis of Hand Evaluation*, 2nd ed.; The Textile Machinery Society of Japan: Osaka, Japan, 1980; pp 24−85.
(27) Sukigara, S.; Dhingra, R. C.; Postle, R. *Text. Res. J.* **1987**, *57* (8), 479−89.
(28) Batoo, M. K.; Kumar, S.; Lee, C. G. *J. Curr. Appl. Phys.* **2009**, *9*, 1397−1406.
(29) Han, H.; Kang, H.; Kim, S.; Kim, H. *J. Power Sources* **2002**, *112*, 461−468.
(30) XPS(X-ray Photoelectron Spectroscopy) Database, http://techdb.podzone.net/. Dynamic Network Services, Inc., Manchester, NH 03101, U.S.
(31) Peng, S. J.; Gao, Z. Q.; Sun, J.; Yao, L.; Wang, C. X.; Qiu, Y. P. *Surf. Coat. Technol.* **2010**, *204* (8), 1222−1228.
(32) Akhter, S.; Zhou, X. L.; White, J. M. *Appl. Surf. Sci.* **1989**, *37*, 201−216.
(33) Briggs, D.; Beamson, G. *Anal. Chem.* **1993**, *65*, 1517−1523.
(34) Gholap, S. H. G.; Badiger, M. V.; Gopinath, C. S. *J. Phys. Chem. B* **2005**, *109*, 13941−13947.
(35) Hirai, T.; Hirai, M.; Osada, Y.; De Ross, D. E. *Polymer Sensors and Actuators*; Springer: Berlin, 2000; Chapter 8, pp 245−257.
(36) Wang, Y. Q.; Zhang, F. Q.; Sherwood, P. M. A. *Chem. Mater.* **1999**, *11*, 2573−2583.